Simultaneous catalytic H$_2$ production and CO$_2$ capture in steam reforming of toluene as tar model compound from biomass gasification

CrossMark

I. Zamboni[a], C. Courson[a,*], D. Niznansky[b], A. Kiennemann[a]

[a] Laboratoire des Matériaux, Surfaces et Procédés pour la Catalyse, LMSPC, UMR 7515, ECPM-Université de Strasbourg, 25 rue Becquerel, 67087 Strasbourg Cedex 2, France
[b] Department of Inorganic Chemistry, Faculty of Natural Sciences of Charles University, Albertov 6, 128 43 Prague 2, Czech Republic

A R T I C L E   I N F O

A B S T R A C T

During biomass gasification in a fast internal circulating fluidized bed (FICFB) reactor hydrogen production is strongly influenced by the physicochemical properties and ability of the catalyst to transform the organic fraction (tar molecules), considered as pollutant and produced along the process. The hydrogen production can be also favored by the sorption of CO$_2$ formed during biomass gasification. In this work, two types of bi-functional sorbents/catalysts were prepared taking into account the high attrition resistance required in this type of reactor. Olivine was chosen as catalyst and support of CaO or CaO–Ca$_{12}$Al$_{14}$O$_{33}$ (CaO–CaAl) used as CO$_2$ sorbent phases. The bi-functional materials and olivine were characterized by SEM, BET, XRD, TPR and Mössbauer spectroscopy. The SEM and BET analyses showed that the higher content of CaO–CaAl on olivine allowed having larger pore volume and smaller pore size than CaO/olivine. XRD and TPR showed that the formation of α-Fe$_2$O$_3$ by oxidation of Fe^{2+} from the olivine structure is favored in presence of the CaO–Ca$_{12}$Al$_{14}$O$_{33}$ phase which improves iron oxide dispersion.

The CaO–CaAl/olivine 1:2 ratio showed the best sorption properties at 700 °C. The CO$_2$ sorption capacity was attributed to the high CaO content and its large pore volume while the presence of Ca$_{12}$Al$_{14}$O$_{33}$ provided CO$_2$ sorption stability during carbonation–decarbonation cycles.
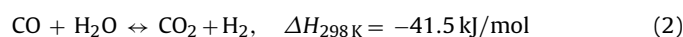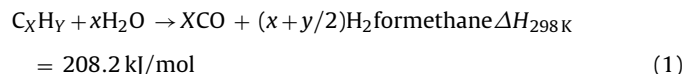
The enhancement of catalytic activity in tar conversion for these bi-functional materials compared to olivine was demonstrated and attributed to the presence of well dispersed iron oxides and the high content of sorbent on olivine surface. This work presents the interest of a CaO–CaAl/olivine catalyst for hydrogen production improved by CO$_2$ capture in a fast internal circulating fluidized bed biomass gasifier.

© 2013 Elsevier B.V. All rights reserved.

1. Introduction

Biomass gasification is often used to supply energy production in a sustainable way by thermo-chemical reactions with steam or oxygen (air) in a synthesis gas mixture (H$_2$ + CO). Those reactions can be promoted by the operating conditions, the design of the reactor but also by the use of appropriated catalysts. Many studies concerning fixed bed reactor have been carried out for biomass gasification [1–6], because of their simplicity in construction and operation [4]. Furthermore, primary catalysts can be designed in fixed bed reactor [7] for fluidized bed [8] or dual fluidized bed reactor [9] use, giving a high biomass conversion. Fluidized bed gasifier (FB) is largely used in small and medium scale (8–100 MV) [10]. In FB reactor, biomass is mixed with a bed material to improve heat exchange, favor fluidization process and then increase conversion. However, with both, steam or oxygen, carbon dioxide and undesirable products as tar are also produced. A practical solution to minimize tar formation is the increase in the reactor temperature; nevertheless the high temperature makes the process expensive and favors the melting of biomass with the ash. To eliminate the tar and increase the process efficiency without an elevated increment of temperature, the tar steam reforming reaction (Eq. (1)) is an interesting way [11] always associated to the water gas shift reaction (WGSR) (Eq. (2)).

$$C_XH_Y + xH_2O \rightarrow XCO + (x+y/2)H_2 \, \text{formethane} \, \Delta H_{298\,K}$$
$$= 208.2 \, \text{kJ/mol} \tag{1}$$

$$CO + H_2O \leftrightarrow CO_2 + H_2, \quad \Delta H_{298\,K} = -41.5 \, \text{kJ/mol} \tag{2}$$

Several researches [8,9,12–14] have been developed to improve FB or FICFB (fast internal circulating fluidized bed) reactors

conditions and decrease tar content. The FICFB reactor consists in two separated zones for gasification and combustion. After the gasification zone, the bed material is transferred to the combustion zone allowing the coke elimination and the bed material regeneration [15]. Rapagnà et al. [16] demonstrated that olivine, a natural mineral, is more promising than dolomite as bed material in a FB reactor because of its high attrition resistance and high efficiency as primary catalyst to reduce the tar level. Olivine is a magnesium and iron orthosilicate, in which the iron is present inside the structure of $(Mg,Fe)_2SiO_4$ as Fe^{2+}. Iron Fe^{3+} can be formed outside of the structure as iron oxide (Fe_2O_3) from oxidation of Fe^{2+} from olivine structure [17]. Iron oxide on the olivine surface plays an important role on the catalytic activity of olivine [3,18,19] by the promotion of the C—C bound breaking for tar conversion, and of the WGSR [20]. Virginie et al. [7] studied catalysts with different contents of iron supported on olivine in steam reforming of toluene and 1-methylnaphthalene chosen as removal reaction of tar model compounds. The optimized iron loading (10 wt%) on olivine showed a high conversion of toluene (90%) at 850 °C in presence of a H_2/H_2O ratio of 1.5. Iron addition on olivine has a high influence on tar conversion.

Olivine has also showed an activity improvement of steam gasification in presence of calcium oxide [21]. Used olivine with a calcium oxide layer produced during gasification and combustion reactions at 850 °C and 930 °C, respectively, has been compared with fresh olivine. Used bed material revealed an enhancement of the exothermic water gas shift reaction (reaction (2)). The H_2 and CO_2 contents were higher while CO decreased. According to those studies it needs to point out that, CO_2 capture in steam reforming of CH_4 [22] and presently of tar is a convenient strategy not only to move on the reforming reaction toward hydrogen production but also to reduce greenhouse gas emissions. In a FICFB gasifier, CO_2 can be captured on a solid sorbent in the gasification zone then concentrated in the flue gas after desorption in the combustion zone. The temperatures of the two zones have to be adapted to this concept.

CaO is also well known as CO_2 sorbent because of its high efficiency in carbonation and calcination reactions [1,23]. However because of the CaO particles agglomeration after calcination its CO_2 sorption stability is reduced after several sorption–desorption cycles. To solve this problem Li et al. [24] synthesized a mixed phase of $CaO–Ca_{12}Al_{14}O_{33}$ and tested different CaO to $Ca_{12}Al_{14}O_{33}$ mass ratios. They observed that higher content of $Ca_{12}Al_{14}O_{33}$ (mayenite) shows higher stability during cycle however has limited sorption capacity because of its low CaO content. They concluded that a mixture of 25 wt% of $Ca_{12}Al_{14}O_{33}$ and 75 wt% of CaO is a convenient composition to have both CO_2 sorption capacity and stability. The $CaO–Ca_{12}Al_{14}O_{33}$ has been largely studied in CO_2 sorption stability during several cycles [25–27]. Manovic and Anthony [25] found that the presence of $Ca_{12}Al_{14}O_{33}$ stabilizes the large number of nanosized pores and that the pellets prepared with this phase are more resistant to sintering and loss of small pores, needed for carbonation. On the other hand the $Ca_{12}Al_{14}O_{33}$ phase has been used as catalyst support. Vagia and Lemonidou [28] tested $Ni/Ca_{12}Al_{14}O_{33}$ in acetic acid reforming. After calcination at 900 °C, nickel particles were incorporated into the bulk of $Ca_{12}Al_{14}O_{33}$ thus decreasing metal surface area and dispersion. Moreover nickel inserted was more difficult to reduce and consequently low activity in acetic acid reforming is observed. In later studies the authors used Ni supported on $CaO/Ca_{12}Al_{14}O_{33}$ in steam reforming of methane at 650 °C [29]. In this case the $Ni–Ca_{12}Al_{14}O_{33}$ interactions were avoided using a high ratio of CaO to Al_2O_3. The authors concluded that $CaO–Ca_{12}Al_{14}O_{33}$ serves not only as an effective support for metallic nickel reforming active sites but also as a CO_2 sorbent with high sorption capacity and excellent stability. $Ni(5 wt\%)/Ca_{12}Al_{14}O_{33}$ has been also used in steam

reforming of toluene between 500 and 800 °C [30]. The catalyst exhibited higher toluene reforming activity, long-time durability and superior resistance to carbon poisoning comparing to commercial $Ni/Ca_x/MgO_{1−x}$.

Even if the calcium oxide can be interesting as catalyst at high temperature [31,32] where the basic sites of calcium oxide are available to the sorption of tar and water [33], in the present study CO_2 sorption process has to be favored. So it is necessary to decrease reaction temperature to perform steam reforming at a temperature as low as possible. According to the CO_2 pressure on calcium oxide at atmospheric pressure [34], carbonation is favored at temperature lower than 700 °C, over this temperature the decarbonation process takes place. It means that if we are interested in steam reforming reaction with simultaneous CO_2 capture the temperature should be limited to the CO_2 sorption conditions. Moreover, if tar could be converted by a metal as iron, less toxic and expensive than nickel at a temperature compatible with CO_2 sorption, then the gasification process becomes environmentally and economically more attractive.

We have designed a CaO or $CaO–Ca_{12}Al_{14}O_{33}$ (CaO–CaAl) on olivine bi-functional material for steam reforming of toluene (tar model molecule) and CO_2 capture. This work is focused on the understanding of its sorption properties and catalytic activity supported by physicochemical properties and catalytic test behavior. The catalysts were designed to be used in FB nevertheless the experiments were carried out in a fix bed reactor to evaluate the properties and catalytic activity under hard conditions.

2. Experimental

2.1. Catalyst preparation

The calcium oxide and aluminium nitrate precursors used in this work were reagent-grade and purchased from Sigma–Aldrich. The olivine was provided by Magnolithe GmbH (Austria) which has improved its mechanical resistance by calcination at 1600 °C. Same olivine has been previously characterized [3,7,35]. The global formula is $(Mg_{0.93}Fe_{0.07})_2SiO_4$ and the grain size used is between 250 and 310 μm.

The CaO sorbent synthesis consisted of a calcination of calcium acetate hydrate ($Ca_2(CH_3COO)_2$) up to 750 °C (3 °C/min) for 4 h. The CaO–CaAl sorbent was prepared basing on the synthesis reported by Martavaltzi and Lemonidou [27]. An aqueous solution of calcium oxide and aluminium nitrate nonahydrate was heated at 70 °C until the salts saturation. The obtained solid was dried then calcined in two stages at 750 °C and then at 900 °C.

Two sorbent/olivine ratios were used (1:2 and 1:4). CaO or CaO–CaAl was deposited on olivine by an aqueous suspension with constant water to sorbent ratio. The suspension is dried and calcined at 750 °C, leading to samples called CaO/olivine 1:2, CaO/olivine 1:4, CaO–CaAl/olivine 1:2 and CaO–CaAl/olivine 1:4. For comparison, olivine was also calcined at 750 °C. The grain size of all sorbents/catalysts and olivine is between 250 μm and 310 μm.

2.2. Characterization

The bi-functional materials were characterized by scanning electron microscopy, BET surface determination, pore distribution analysis, X-ray diffraction, temperature programmed reduction and Mössbauer spectroscopy.

2.2.1. Scanning electron microscopy

Scanning electron microscopy (SEM) micrographs were recorded on a JEOL 6700F microscope working at 15 kV accelerating voltage in order to study the morphology of the sorbents/catalysts.

2.2.2. BET

A Micromeritics Tristar 3000 surface area and pore distribution analyzer was employed for measurement of BET surface area by recording the nitrogen adsorption and desorption isotherms at 196 °C (77 K). The catalysts were previously degassed at 250 °C for at least 3 h.

2.2.3. X-ray diffraction

X-ray diffraction pattern of sorbents/catalysts was recorded on an X-ray diffractometer Brucker AXS D8 advanced using CuKα radiation to identify the crystalline phases. The diffraction spectra have been indexed by comparison with the joint committee on powder diffraction standards (JCPDS) files.

2.2.4. Temperature programmed reduction

The reducibility of sorbents/catalysts under hydrogen was carried out on 100 mg of material. First, decomposition of possible carbonates was performed from room temperature to 750 °C under argon. Then after the cooling of the sorbent/catalyst until room temperature the reductive gas mixture (10 vol% H_2 in Ar) passed through the reactor heated from room temperature to 1000 °C with a slope of 15 °C/min then maintained at 1000 °C for 30 min. A thermal conductivity detector (TCD) permitted the quantitative determination of hydrogen consumption.

2.2.5. Mössbauer spectroscopy

The Mössbauer measurements were carried out in transmission mode with ^{57}Co diffused into an Rh matrix as a source moving with constant acceleration. The spectrometer (Wissel) was calibrated by means of a α-Fe foil standard, and the isomer shift was expressed with respect to this standard at 293 K. The fitting of the spectra was performed with the help of the NORMOS program.

2.3. Sorption properties

Several studies have showed that CO_2 sorption properties of CaO depend of some parameters as calcium oxide precursors, preparation method, temperature rate, etc. According to diverse studies, Grasa and Abanades [36] have concluded that a large decrease in carbonation capacity of CaO can occur after 20 cycles. Afterwards, one of the most important challenges is to prepare calcium oxide sorbent with high sorption capacity and sorption stability after several carbonation and decarbonation cycles. Studies regarding to the CaO sorption stability [25,26] have shown the importance of $Ca_{12}Al_{14}O_{33}$ (mayenite) phase to avoid sintering and sorption decay after several cycles.

In this work calcium oxide previously optimized from calcium acetate precursor, was associated with the calcium aluminates (mayenite) phase to avoid sintering and improve stability. The sorption tests were carried out to evaluate the percentage of sorption capacity and the desorption temperature of CaO and CaO–CaAl deposited on olivine and to verify the sorption stability after seven cycles.

2.3.1. Sorbent capacity

The sorption tests were carried out with 100 mg of sorbent/catalyst by using a fixed bed reactor (6 mm of inner diameter). The total flow of 3 L/h contains CO_2 (10 vol%) in helium and was controlled by mass flow controller. The sorption tests were performed in 4 steps. During the first step, the sorbent was heated until 800 °C under helium in order to remove CO_2 and water molecules accumulated on the surface during the storage. After cleaning the temperature was fixed at 700 °C. Taking into account the CO_2 pressure on calcium oxide at atmospheric pressure diagram [34], Eq. (1) and the minimum temperature for tar reforming [21,37], the chosen temperature corresponds to the maximum temperature

where CO_2 sorption still possible. The CO_2 sorption step was started (step 2): the CO_2 gas mixture passed through the sorbent during 1 h. After the sorption step, the CO_2 gas mixture was switch to He (3 L/h) and the temperature was increased from 700 °C until 800 °C with a heating rate of 5 °C/min to carry out the CO_2 desorption (step 3). The desorption was carefully followed by TCD until total released of CO_2. The total desorption of CO_2 is then equivalent to the total CO_2 that could be captured/trapped during the sorption step (step 2).

2.3.2. Thermo-gravimetric analysis

In order to schematize the CO_2 capture in the gasification zone and the CO_2 desorption in the combustion zone, the carbonation and decarbonation experiments were performed with a thermo-gravimetric analyzer (TGA Q5000, TA Instruments) and permit to study the CO_2 sorption stability. Thermo-gravimetric analysis was carried out in the same conditions mentioned before to determinate the sorption capacity, however the initial weight sample was between 5 mg and 10 mg and the total flow of 0.3 L/h according to the TGA equipment characteristics.

The realistic gas mixture in the combustion zone (regeneration) contains air, but no H_2O and, very low CO_2 concentration (about 2.6%) [9]. In this work, the desorption was performed under He atmosphere, which corresponds to more severe conditions than the actual conditions. To assure the maximal desorption of CO_2 and minimize the sintering, the maximum temperature chosen for the desorption step was 800 °C.

2.4. Catalytic tests

Catalytic activity in tar removal was evaluated in a fixed bed reactor by steam reforming of toluene as tar removal model reaction The fixed-bed quartz reactor (inner diameter 8 mm) containing sorbent/catalyst bed (500 mg) supported by quartz wool was placed in a furnace in which the heating is monitored by a thermocouple. Using two independent channels from HPLC pumps, water and toluene were introduced into a vaporization furnace (250 °C) and then carried to the reactor by a flow (total flow of 3 L/h) containing a mixture of argon (carrier gas) and nitrogen (internal standard) (GHSV: 7500 h^{-1}). Toluene concentration (10 g/N m^3) was chosen in order to perform catalytic tests in conditions similar to those observed in a biomass fluidized bed gasifier (about 2–10 g/N m^3) [38]. Stoichiometric H_2O/C_7H_8 ratio (14/1) was established according to Eq. (3), herein steam reforming and water gas shift reaction are involved (Eqs. (1) and (2)). The gas mixture consists of 0.13 mL/min of toluene (0.27 vol%), 1.86 mL/min of H_2O (3.72 vol%) and 48 mL/min of Ar, according to this conditions the S/C ratio is around 2.

$$C_7H_8 + 14H_2O \rightarrow 7CO_2 + 18H_2 \qquad (3)$$

The catalytic tests were carried out for 4 h. The gas leaving the reactor was analyzed continuously by three gas chromatographs. Delsi Instruments Di200 and Agilent 7890A gas chromatographs equipped by TCD were used to analyze CO_2, H_2, CO, CH_4, N_2 and a Varian star 3400 CX gas chromatograph equipped by FID detector was employed to quantify heavy molecules as toluene, benzene and CxHy.

3. Results and discussion

3.1. Characterization

3.1.1. SEM

The sorbents/catalysts and fresh olivine were analyzed by scanning electron spectroscopy in order to evaluate the morphology
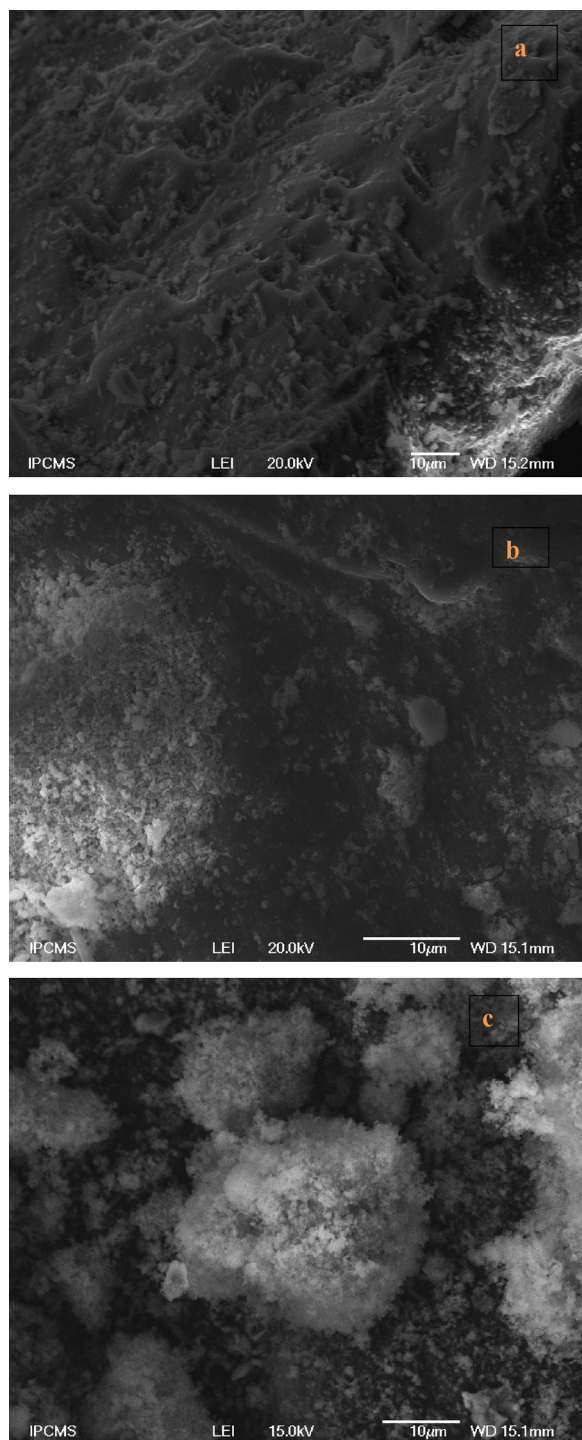
Fig. 1. SEM micrographs of (a) fresh olivine, (b) CaO–CaAl/olivine 1:4 and (c) CaO–CaAl/olivine 1:2.

of the olivine surface after the addition of different contents of sorbent. The Fig. 1 shows SEM micrographs of olivine, CaO–CaAl/olivine 1:4 and CaO–CaAl/olivine 1:2. In Fig. 1a it can be seen that olivine has a smooth surface. After deposition of small quantity of sorbent (1:4 ratio) the olivine is partially covered by the CaO–CaAl sorbent (Fig. 1b). By contrast, when more quantity of sorbent is added (1:2 ratio) the particles of the sorbent are bigger but quite well dispersed on the surface of olivine.

Table 1
BET surface area, pore volume and average pore size of sorbent/catalyst materials.

Sorbent/catalyst materials	BET (m^2/g)	Pore volume (cm^3/g)	Average pore size (nm)
Olivine (750 °C)	<1	–	–
CaO	11.3	0.042	50.6
CaO–CaAl	9.3	0.025	11.6
CaO/olivine 1:2	4.5	0.014	14.6
CaO–CaAl/olivine 1:2	8.8	0.023	11.8
CaO/olivine 1:4	1.6	0.002	25.9
CaO–CaAl/olivine 1:4	2.5	0.004	17.8

3.1.2. BET surface area

According to the very low surface area of olivine (Table 1), it appears that the surface area of sorbents/catalysts is due to the presence of the sorbent phase. The surface area of sorbents decreases when deposited on olivine (due to the calcination step) until reaching values close to that of olivine for the lowest sorbent/olivine ratio. This agrees with SEM results which conclude that the sorbent covers a few part of olivine surface.

In sorbents/catalysts with 1:2 ratio the surface area of CaO/olivine is largely lower than the CaO surface while the CaO–CaAl/olivine surface is comparable to the CaO–CaAl one. It seems that the presence of the $Ca_{12}Al_{14}O_{33}$ (mayenite) phase stabilizes CaO with a partial preservation of its surface area after deposition on olivine. Martavaltzi and Lemonidou [29] observed that surface area of NiO/CaO–$Ca_{12}Al_{14}O_{33}$ decreases with nickel loading. In our case, the content of iron on the olivine surface increasing after calcination [10] could also lead to the decreasing surface area of the sorbents.

The average pore size of all sorbents/catalysts was established in the range of mesoporous materials (Table 1). After deposition on olivine, CaO has smaller pore volume; this phenomenon confirms the sintering effect of calcination.

Concerning the effect of the $Ca_{12}Al_{14}O_{33}$ phase, the results again suggest that its addition favors the stability of CaO deposited on olivine because its pore size and volume do not change after deposition step on olivine for the 1:2 ratio. The differences observed between the both sorbent/olivine ratios could be explained by a higher rate of water evaporation with the 1:4 ratio associated to the lower water amount. In fact, large pores could be formed during evaporation with slow rates.

Abanades and Alvarez [39] associated the sorption capacity loss to the increase of pore size. Regarding to the influence of surface area and pore volume, Lu and Smirniotis [40] have concluded that calcium oxide sorbent with high surface area and large pore volume demonstrated faster kinetics and larger capacity of carbonation. In this connection, our results suggest that CaO/olivine and CaO–CaAl/olivine 1:2 are convenient materials to favor CO_2 sorption especially when the $Ca_{12}Al_{14}O_{33}$ (mayenite) phase is present, because of the large pore volume and small pore size of CaO compared to the sorbent without the binder phase.

3.1.3. X-ray diffraction

XRD patterns of olivine, calcined olivine (750 °C), CaO/olivine 1:4 and CaO–CaAl/olivine 1:4 are presented in Fig. 2. Orthorhombic structure of forsterite Mg_2SiO_4 (JCPDS 34-0189), the main phase of olivine (Fig. 2 spectrum a) is identified in all samples ($2\theta = 35.8°$, $36.6°$, $39.7°$ and $40.1°$). The rays at $2\theta = 37.4°$ and $41.2°$ (Fig. 2 spectrum c and d) matches well to the cubic structure of CaO (JCPDS 70-4068) and to the mayenite $Ca_{12}Al_{14}O_{33}$ (JCPDS 09-0413) phase, respectively. After calcination of olivine (spectrum b) or in presence of CaO–CaAl (spectrum d), the α-Fe_2O_3 phase is clearly observed ($2\theta = 33.2°$) while the only iron phases detected on olivine XRD pattern are γ-Fe_2O_3 ($2\theta = 35.7$) or Fe_3O_4/$MgFe_2O_4$ (spinel) ($2\theta = 35.6°$) and ε-Fe_2O_3 ($2\theta = 32.9°$). The latter is a transition phase between γ

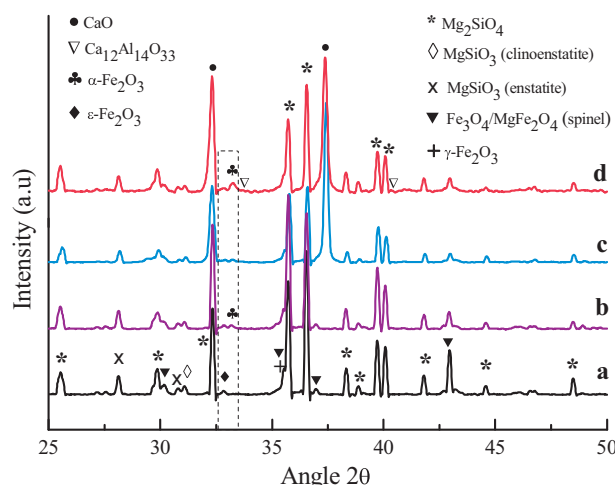**Fig. 2.** X-ray diffractograms of (a) olivine, (b) olivine (750 °C), (c) CaO/olivine 1:4 and (d) CaO–CaAl/olivine 1:4.

Fig. 3. TPR profiles of (a) olivine, (b) CaO/olivine 1:4 and (c) CaO–CaAl/olivine 1:4.

and α stabilized by the SiO_2 matrix [41]. Regarding to those results, the formation of α-Fe_2O_3, by oxidation of Fe^{2+} from forsterite structure to Fe^{3+}, is likely promoted in the bulk by the calcination in presence of CaO–CaAl.

Particle size calculated from Debye–Scherrer formula can provide information about oxide dispersion on the support surface. In Table 2 the particle size of catalyst and sorbent raw materials (olivine, CaO and CaO–CaAl) and of sorbent/catalyst systems are reported. The deposition of CaO sorbent on olivine did not modify its particle size. The $Ca_{12}Al_{14}O_{33}$ addition as a binder phase has a positive effect toward the formation of smaller particles of CaO deposited on olivine.

On the other hand, the iron oxide particles present on CaO–CaAl/olivine or CaO/olivine have in general, smaller size compared to iron oxide particles characterized on olivine calcined at the same temperature (Table 2). No significant effect of $Ca_{12}Al_{14}O_{33}$ addition on the iron particles size can be seen with the sorbent/catalyst 1:2, however, the decrease in the iron particles size is very clear in the case of the 1:4 ratio (Table 2). The size of those particles suggests that dispersion of iron oxide can be improved during the synthesis process in presence of the mayenite phase. It can be considered that the iron phases are better dispersed on the sorbent when a small quantity of $Ca_{12}Al_{14}O_{33}$ is present.

3.1.4. Temperature programmed reduction

Temperature programmed reduction measurements were carried out to identify the iron species and their reducibility under temperature of steam reforming reaction. Iron oxide reduction pathway depends of many different parameters [42–44]. For this reason the TPR analysis are supported over the comparison at the

same conditions and also on DRX results. The general reduction profile of iron oxide corresponds to the following reactions:

$$Fe_2O_3 \rightarrow Fe_3O_4 \rightarrow FeO \rightarrow Fe^0$$
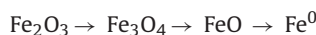
However olivine structure presents more complex reduction process previously described by Swierczynski et al. [17] and illustrated below.

$$\underset{\text{Hematite}}{\alpha\text{-}Fe_2O_3} + \underset{\text{Magnesionfernite}}{MgFe_2O_4} \xrightarrow{\text{Reduction } 950\,°C} Fe^0 + Fe^{2+} + MgO \xrightarrow{Mg_2SiO_4} Fe^0$$

$$+ (Mg, Fe)_2SiO_4 + MgO$$
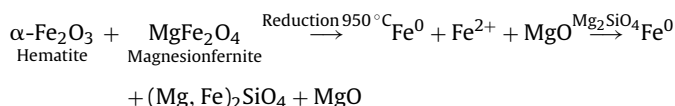
Olivine reduction profile (Fig. 3a) shows a wide reduction peak which suggests that the reduction steps are overlaps and take place in a wide range of temperature. However, a shoulder at 500 °C can be assigned to the reduction of α-Fe_2O_3 to Fe_3O_4 followed by the reduction step of Fe_3O_4 to FeO and Fe^0, around 630 °C. The metallic iron phase observed by XRD after temperature programmed reduction (data no showed) confirms that under reductive conditions, all the oxidation states can be obtained by reduction of the various iron species observed by XRD in the fresh olivine sample. The reduction zone at high temperature (900 °C) could be attributed to the reduction of iron species in $MgFe_2O_4$ more difficult to reduce [17].

According to the profile of CaO/olivine 1:4 and CaO–CaAl/olivine (Fig. 3b and c), it can be observed that the presence of the sorbent phase does not have significant effect on the reduction pathway of iron species. The sorbents/catalysts 1:2 showed similar behaviors of α-Fe_2O_3 to Fe^0 reduction.

The reduction temperature and iron reduction percentage of sorbents/catalysts are summarized in Table 3. Iron reduction percentages are quite similar to those obtained with olivine when a small quantity of calcium oxide is present. By contrast, the percentage of iron reduction decreases as the percentage of calcium oxide increases. That can be explained by two phenomena. Firstly, iron particles are protected by calcium oxide layer which limits H_2 access, the SEM micrographs showed that olivine surface is

Table 2
Particle size calculated from X-ray diffractograms of sorbent/catalyst materials.

Sorbent/catalyst materials	CaO particles size (nm) ±1 nm	Fe_2O_3 particles size (nm) ±1 nm
Olivine	–	46
Olivine (750 °C)	–	47
CaO	36	–
CaO–CaAl	37	–
CaO/olivine 1:2	35	38
CaO–CaAl/olivine 1:2	31	40
CaO/olivine 1:4	40	44
CaO–CaAl/olivine 1:4	34	29

Table 3
Iron reduction percentage and reduction temperature of sorbents/catalysts.

Sorbent/catalyst	Iron reduction (%)	Reduction temperature (°C)
Olivine	20	623
CaO/olivine 1:2	17	616
CaO–CaAl/olivine 1:2	10	623
CaO/olivine 1:4	22	628
CaO–CaAl/olivine 1:4	22	619
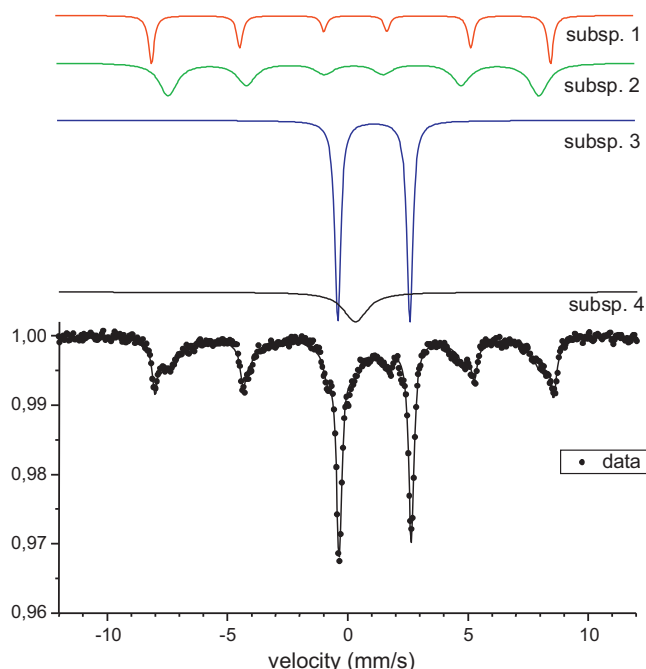
Fig. 4. ^{57}Fe Mössbauer spectra and subspectra at 77 K of CaO–CaAl/olivine 1:4.

Fig. 5. Sorption test of (▬▬▬) CaO–CaAl/olivine 1:2, (▬▬▬) CaO/olivine 1:2, (▬▬▬) CaO–CaAl/olivine 1:4 and (▬▬▬) CaO/olivine 1:4.

more covered when sorbent/catalyst ratio is 1:2. Secondly, the calcium oxide limits the iron oxidation from $(Mg,Fe)_2SiO_4$ structure to hematite and consequently there is less iron available to be reduced in H_2 atmosphere compared to sorbents/catalysts with 1:4 ratio.

3.1.5. Mössbauer spectroscopy

In order to better understand how the sorbent phase affects the formation of iron species on olivine, Mössbauer spectroscopy analyzes were carried out. The CaO–CaAl/olivine 1:4 was analyzed by Mössbauer spectroscopy (Fig. 4) because the XRD results showed a particular behavior of iron species in this sorbent/catalyst. The parameters of iron species in this sorbent/catalyst are compared with those observed in fresh olivine [17] (Table 4).

Fig. 4 shows two sextets (subsp. 1 and 2). The parameters of the subsp. 1 correspond to Fe^{3+} in hematite phase (α-Fe_2O_3). This phase was clearly identified by XRD and TPR in the CaO–CaAl/olivine sorbent/catalyst. On the other hand, the subsp. 2 is assigned to γ-Fe_2O_3 or magnesioferrite ($MgFe_2O_4$). In fact, γ-Fe_2O_3 and magnesioferrite have the same spinel structure. The γ-Fe_2O_3 has only one broad sextet because of the superposition of tetrahedral and octahedral iron and influence of the structure with vacancies. Pure magnesioferrite is normal spinel having Mg only in tetrahedral position and Fe in octahedral position thus spectra will have only one sextet below Neel temperature (above Neel temperature will be paramagnetic behavior and doublet in Mössbauer spectra). Nevertheless, some disorder and effect of small particles could be present, and then one sextet will be observed at room temperature [45].

The subsp. 3 shows a doublet (hyperfine parameters $IS_{Fe} = 1.14$ mm/s and $Qs = 3.0$ mm/s) which corresponds to Fe^{2+} in octahedral sites of olivine structure.

The subsp. 4 which corresponds to the Fe^{3+} in paramagnetic compound was not previously observed in olivine (in fresh olivine or even in calcined olivine) [7,17]. It suggests that small paramagnetic particles of Fe^{3+} are formed from the oxidation of Fe^{2+} of the olivine structure in presence of the CaO–CaAl phase. The presence of small iron oxide particles has been also observed by X-ray diffraction.

The percentage of α-Fe_2O_3 and γ-Fe_2O_3 phases are slightly higher in CaO–CaAl/olivine than in olivine. The percentage of Fe^{2+}
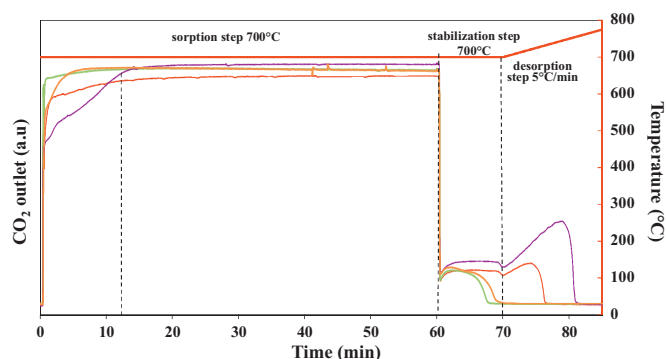
in the olivine structure is lower in CaO–CaAl/olivine than in olivine. Those results clearly confirm the oxidation of Fe^{2+} to Fe^{3+} during the synthesis of CaO–CaAl/olivine.

To summarize, the surface characterization of the sorbents/catalysts by SEM and BET showed that when sorbent/catalyst ratio is 1:2, the sorbent are quite well deposited on olivine with the highest pore volume and the smallest pore size. XRD and TPR showed that α-Fe_2O_3 is present in all sorbents/catalysts. TPR confirmed that the formation of Fe^{3+} from olivine is favored in presence of small quantities of sorbents (1:4 ratio). The quantitative analysis by Mössbauer spectroscopy showed that the principal iron species present in sorbent/catalyst 1:4 are α-Fe_2O_3, γ-Fe_2O_3/$MgFe_2O_4$ spinel phase and a new paramagnetic iron phase not previously observed on olivine.

The addition of the mayenite phase in significant amount (1:2 ratio) stabilizes the calcium oxide in term of porosity and in lower amount (1:4 ratio) favors iron oxide dispersion.

3.2. Sorption properties

3.2.1. Sorption capacity

Fig. 5 shows the sorption profile of the sorbents/catalysts. Three steps are observed; (1) CO_2 sorption at 700 °C, (2) desorption-stabilization at 700 °C and (3) total desorption with a temperature ramp.

(1) In the first step the sorbents/catalysts reach an equilibrium value. However, this process is divided in two stages. In the case of CaO–CaAl/olivine 1:2 the pores of the sorbent are quickly saturated by CO_2 that leads to the formation of a $CaCO_3$ layer. After the first minutes, the second stage starts with the diffusion of CO_2 through the saturated layer, this stage has been defined by several authors as diffusion controlled regime. This sorption behavior is suitable for cyclic reactions because the sorbent can be regenerate quickly after saturation. In the case of CaO/olivine 1:2, the behavior is different; the first stage is slowly which suggests that CO_2 takes more time to fill the pores. It can be probably caused by the smaller pore volume of CaO/olivine compared to the pore volume of CaO–CaAl/olivine as observed by BET analysis. In this case the diffusion through the $CaCO_3$ layer is later reached. For the sorbents/catalysts 1:4, these phenomena are less significant because the sorbent quantity is lower and the pore volume is smaller.

(2) During the 10 min of the stabilization (second step) at 700 °C under 100% of helium, the sorbents/catalysts 1:2 partially release the CO_2 previously trapped. In contrast the sorbents/catalysts 1:4 totally desorbs the CO_2. The sorption capacity of those bi-functional materials was not higher than 8% which can be related to its small pore volume and large pore

Table 4
^{57}Fe Mössbauer parameters of the iron species present in olivine and CaO–CaAl/olivine 1:4 (sorbent/olivine).

Interpretation		Isomer shift δ (mm/s)		Quadrupole splitting ΔE_Q (mm/s)		Hyperfine field B_{HF} (kG)		Relative area (%)	
		Olivine	Sorbent/olivine	Olivine	Sorbent/olivine	Olivine	Sorbent/olivine	Olivine	Sorbent/olivine
Subsp. 1	Fe(3+) in hematite	0.36	0.37	0.00	−0.19	518	515	14	17
Subsp. 2	Fe(3+) in γ-Fe$_2$O$_3$	0.26	0.34	0.00	−0.01	495	479	31	37
Subsp. 3	Fe(2+) paramagnetic (olivine structure)	1.12	1.14	3.06	3.00	0	0	55	36
Subsp. 4	Fe(3+) paramagnetic	0	0.30	0	0.01	0	0	0	10

size. These results suggest that in tar steam reforming at 700 °C, the sorbent/catalyst 1:4 ratio is not able to provide sufficient CO$_2$ sorption capacity.

(3) In the third step, the CaO/olivine 1:2 and CaO–CaAl/olivine 1:2 reach a maximum desorption temperature around 720 and 740 °C, respectively and the whole CO$_2$ is finally desorbed. The higher desorption temperature observed with sorbents/catalysts 1:2 indicates stronger interactions between CO$_2$ and the sorbent and then more important sorption phenomenon which can be attributed to the larger pore volume. The CaO/olivine 1:2 has more sorption capacity than CaO–CaAl/olivine 1:2 however the performance in cyclic reaction could be limited by its longer time of saturation in the first minutes of the sorption step.

According to sorption capacity and desorption temperature at 700 °C (temperature of the tar steam reforming in this work), the CO$_2$ sorption on CaO/olivine and CaO–CaAl/olivine 1:2 should have a positive effect on the H$_2$ production.

3.2.2. Thermo-gravimetric analysis

The thermo-gravimetric analyzes (TGA) were carried out to evaluate the sorption capacity and stability of CaO/olivine and CaO–CaAl/olivine 1:2. The weight change (% relative to the initial weight of sample) of sorbents/catalysts 1:2 is evaluated as a function of carbonation–decarbonation cycles (Fig. 6). Those two sorbents/catalysts have almost the same sorption capacity (26.3 wt% in the first cycle) but during 7 cycles of carbonation–decarbonation CaO–CaAl/olivine is more stable (loss of less than 0.2% of its initial sorption capacity) than CaO/olivine (loss of 9%). According to Alvarez and Abanades [46] the development of a thin shell in the outer surfaces of a calcined sorbent, made up of small CaO grains that leave between small pore prone to blockages during carbonation. This phenomenon is activated by the long carbonation times (30 min) in the first carbonation cycles and produces the loss of sorption capacity. Additionally, the CaCO$_3$

molar volume (36.9 cm^3/mol) is higher than the CaO molar volume (16.9 cm^3/mol). This means that when calcium carbonate is formed its layer thickness fills the CaO pore volume; and then the rest of the layer thickness will cover the neighboring pores. In the case of CaO/olivine and CaO–CaAl/olivine 1:2, the pore size is small and very similar, however the pore volume of CaO–CaAl/olivine 1:2 is a double of CaO/olivine pore volume. So the pore volume of the neighbors will be less filled by the layer thickness of carbonate. The latter and the fact that CaAl network maintains the CaO particles disjointed can minimize the blockage effect in small pores. The sorbents/catalysts with 1:4 ratio show similar behavior (data not shown) however because of the sorbent dilution in the samples the sorption is less significant. This clearly show that the addition of Ca$_{12}$Al$_{14}$O$_{33}$ in the sorbent/catalyst gives the possibility to carry out tar steam reforming with regeneration cycles without significant decrease in the sorption properties of CaO.

Several works [25,26,47–49] indicated that the presence of Ca$_{12}$Al$_{14}$O$_{33}$ phase stabilizes the CO$_2$ sorption capacity of CaO after multiple cycles of sorption–desorption. Here it is additionally demonstrated that impregnation of CaO–CaAl on olivine does not affect the performance of Ca$_{12}$Al$_{14}$O$_{33}$ used as a binder for CaO. It means that the performance of CaO/olivine catalyst in sorption–desorption cycles can be improved using mayenite phase.

The CO$_2$ sorption stability of the CaO–CaAl/olivine 1:2 after catalytic test was confirmed by thermo-gravimetric analysis during 30 cycles of carbonation–calcination (Fig. 7). The sorption capacity at the end of 30 cycles, when the sorption stability has been attainted is 8.6% less of the initial sorption. This is considered as a good stability considering that the sorbent material has been exposed to the steam reforming gas mixture.

3.3. Catalytic tests

Steam reforming of toluene was carried out at 700 °C in order to evaluate the catalytic behavior of sorbent/catalyst materials. The catalytic effect of each component of the material (sorbent and
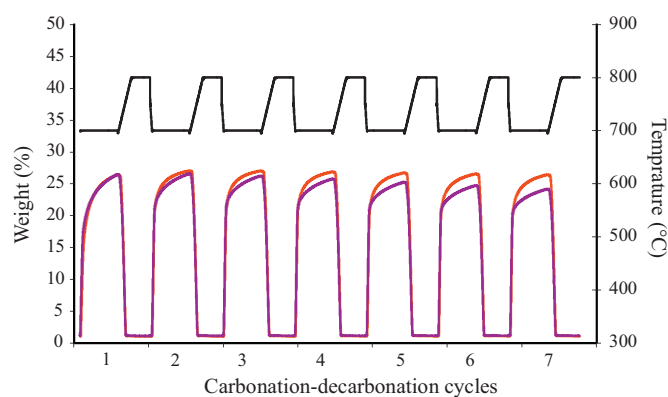

Fig. 6. TGA analyses: CO$_2$ sorbent capacity during carbonation–decarbonation cycles of (━ ━ ━). CaO/olivine 1:2 and (━ ━ ━) CaO-CaAl/olivine 1:2. (—) Represent the temperature ramp.
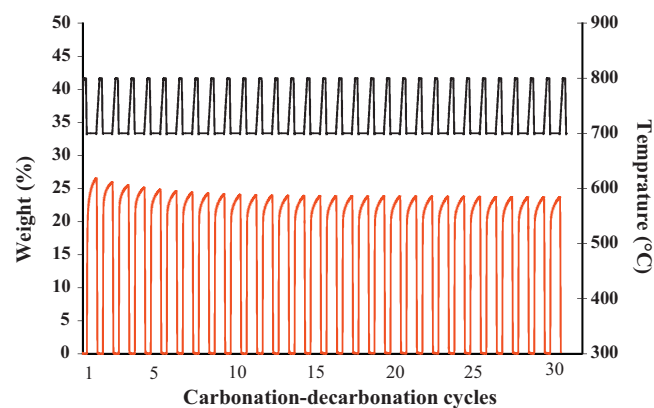

Fig. 7. TGA analyses: CO$_2$ sorbent capacity during 30 carbonation–decarbonation cycles of (━ ━ ━) CaO–CaAl/olivine 1:2 after catalytic test. (—) Represent the temperature ramp.

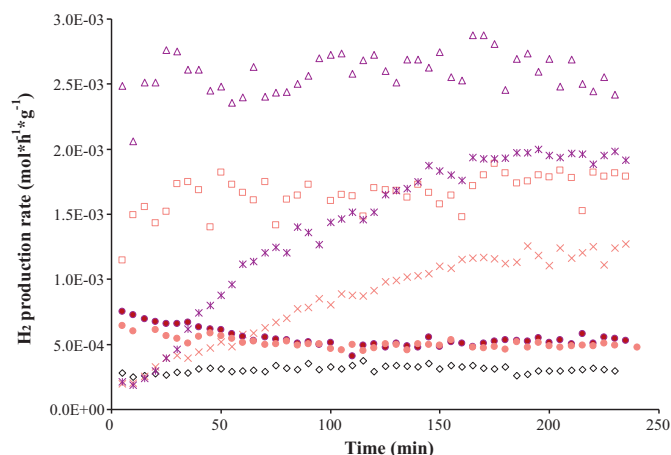**Fig. 8.** Catalytic behavior of ($\diamond$) olivine, ($*$) CaO, ($\times$) CaO–CaAl, ($\bullet$) CaO–CaAl/olivine 1:4 and ($\bullet$) CaO/olivine 1:4, ($\square$) CaO–CaAl/olivine 1:2 ($\triangle$) CaO/olivine 1:2.

Fig. 9. CO$_2$ selectivity of ($\diamond$) olivine, ($*$) CaO, ($\times$) CaO–CaAl, ($\bullet$) CaO–CaAl/olivine 1:4 and ($\bullet$) CaO/olivine 1:4, ($\square$) CaO–CaAl/olivine 1:2 ($\triangle$) CaO/olivine 1:2.

catalyst) on the activity was evaluated following the H$_2$ production rate and CO$_2$ selectivity.

Fig. 8 shows that olivine has low activity in tar steam reforming at 700 °C. In the case of calcium oxide, the H$_2$ production rate increases slowly until to reach a stable value after 2 h of reaction. At the end of the reactivity tests (4 h) its activity is six times higher than that of olivine. In the case of CaO–CaAl a superior performance in tar steam reforming than olivine is also observed. According to these results it can be ensure that in our conditions, calcium oxide favors H$_2$ production in toluene steam reforming.

In Fig. 8 the catalytic activity of sorbents/catalysts 1:4 was compared to the references (olivine, CaO and CaO–CaAl). At the beginning (first 30 min of reaction), the sorbents/catalysts reach their maximum H$_2$ production rate (2.7 times more active than raw materials) which is ideal for a use in dual fluidized bed reactor. Then they stabilize and remain active (1.6 times more than olivine) during 4 h. In this period the activity of the sorbents surpasses sorbent/catalyst materials. The initial activity of sorbents/catalyst 1:4 may be attributed to the reduction of hematite phase on their surface. Taking into account the characterization results:

- The particle size of α-Fe$_2$O$_3$ obtained by XRD is smaller in sorbents/catalyst 1:4 than in olivine sample calcined at 750 °C, then the greatest dispersion can be related to the best activity.
- Mössbauer spectroscopy showed higher content of Fe$_2$O$_3$.

The stabilization step can be attributed to the reduction of small Fe^{3+} paramagnetic particles which are produced from olivine only in presence of sorbent.

In order to evaluate the effect of the quantity of the sorbent deposited on the olivine surface, CaO/olivine 1:2 and CaO–CaAl/olivine 1:2 sorbents/catalysts were tested in tar steam reforming and compared in terms of hydrogen production rate to olivine, CaO and CaO–CaAl (Fig. 8).

CaO/olivine 1:2 and CaO–CaAl/olivine 1:2 have higher activity (6 times more) than CaO and CaO–CaAl from the beginning of the reaction and still stable during 4 h. CaO/olivine shows better activity than CaO–CaAl/olivine which is consistent with the higher percentage of iron reduction in CaO/olivine 1:2 than in CaO–CaAl/olivine 1:2 determined by TPR. The hydrogen production efficiency of these two materials was calculated taking into account the average value of H$_2$ rate production (from Fig. 7), the inlet toluene concentration (10 g/Nm^3), the mass of bed material (0.5 g) and the total flow (3 L/h). The CaO–CaAl/olivine 1:2 and CaO/olivine 1:2 reported a H$_2$ production efficiency of 13% and 22%, respectively. It is clear that these H$_2$ production efficiencies are lower than those obtained
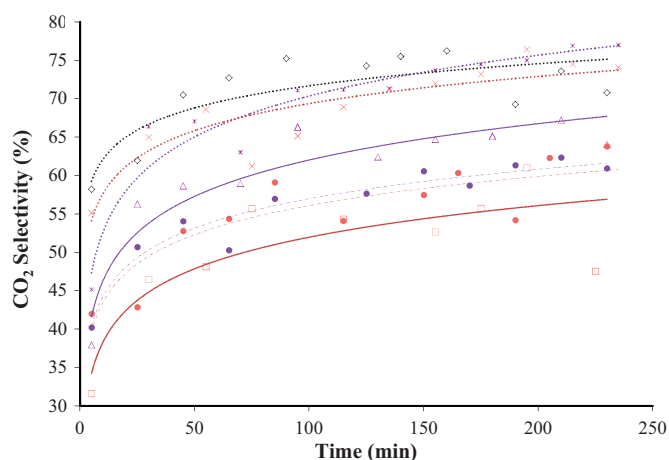
in fixed bed reactor at high temperatures, using others tar catalysts as iron/olivine [7] or nickel/olivine [3]. Olivine can be also associated with calcium to improve its activity in biomass conversion above 800 °C [21]. Besides, the 4% Ni/(Ca,Mg)O (4% Ni/calcined dolomite) catalyst has been used in fixed bed reactor for toluene steam reforming and CO$_2$ capture at 650 °C [1]. Thanks to CO$_2$ sorption, total conversion was observed which decreases to 85% after saturation of the dolomite. In this work, the sorbent/catalyst activity is attributed to the nickel content. In our work, calcium/olivine based catalysts were used to profit of the olivine iron content and attrition resistance.

The efficiency of the reaction could be improved by an increase in temperature. But one of our objectives was to minimize the energy of the process by coupling steam reforming and CO$_2$ capture at low temperature. Even if iron is less active than nickel, its environmental impact is lower. Another objective was the design of a material to be used as primary catalyst to reduce tar content in the product gas before going through to the filters candles, commonly used in FB reactors.

In this purpose, taking into account the low temperature used for the steam reforming of toluene (700 °C), the H$_2$ production efficiency seems promising. The fact that the CaO–CaAl/olivine or CaO/olivine 1:2 showed better activity and stability than olivine in critical conditions for tar reforming (low temperature, low mass transfer) opens the possibility to use these materials in fluidized bed reactor at temperatures below 800 °C.

Fig. 9 shows the CO$_2$ selectivity of the sorbents/catalysts and the raw materials. Olivine presents the highest percentage of CO$_2$ selectivity (60%). In the first minutes of reaction the CaO and CaO–CaAl have low CO$_2$ selectivity and then they quickly reach high CO$_2$ selectivity values as olivine. In the case of olivine, the selectivity of CO$_2$ only depends on its activity because it presents no sorption capacity. However in the case of sorbents, the CO$_2$ selectivity depends on the activity in steam reforming then on CO$_2$ production but also on the CO$_2$ sorption capacity. This latter phenomenon leads to the shift of the water gas shift reaction toward H$_2$ production and CO$_2$ increases (Le Chatelier principle).

The presence of CaO or CaO–CaAl on olivine (ratios 1:4 and 1:2) decreases the CO$_2$ selectivity compared to the raw materials. The lower CO$_2$ selectivity and higher H$_2$ production than olivine demonstrate their quite good catalytic activity and the effect of CO$_2$ sorption on the equilibrium of the water gas shift reaction. However those two phenomena are observed at the same time only for CaO–CaAl/olivine 1:2. This material leads to one of the highest hydrogen production (Fig. 8) which could be associated to the CO$_2$

sorption. In fact, its CO_2 selectivity is the lowest for the whole test duration. These results suggest that the addition of the CaO–CaAl sorbent to olivine stabilizes the high CO_2 sorption which implies a large enhancement of the H_2 production rate during the tar steam reforming at 700 °C.

According to the catalytic activity tests, a synergy between the active phase in olivine and the sorbent phase is highlighted in the bi-functional material leading to promising performances in tar steam reforming.

4. Conclusion

This study shows the effect of the addition of CaO or CaO–CaAl on olivine using to different ratios of sorbent on olivine. The characterizations allowed establishing two behaviors. First, in presence of high quantities of CaO–CaAl (1:2 ratio), the bi-functional material showed the best textural properties (BET, pore volume, pore size). Secondly in presence of low quantities of CaO–CaAl sorbent (1:4 ratio), the Fe^{2+} from olivine structure is more easily oxidized to Fe^{3+}. Mössbauer spectroscopy demonstrated the presence of different kinds of iron Fe^{3+} formed from the oxidation of Fe^{2+} present in olivine structure. The α-Fe_2O_3 and the γ-Fe_2O_3 or $MgFe_2O_4$ phase are present in high quantities and a trivalent iron in paramagnetic compound, which is attributed to small particles of α-Fe_2O_3 is also observed.

The CO_2 sorption of CaO and CaO–CaAl deposited on olivine are governed by different phenomena sorption. As a result of larger pore volume, the CaO–CaAl has a higher sorption rate and consequently a faster saturation rate than CaO in the first minutes of sorption. The CO_2 sorption tests show that the sorbent to catalyst ratio 1:2 is the appropriate ratio to favor the strong interactions between CO_2 and sorbent at 700 °C. Thermo-gravimetric analyzes were performed to evaluate the CO_2 sorption stability during several carbonation–decarbonation cycles. It was observed that the CO_2 sorption stability of the CaO–CaAl/olivine is better than for CaO/olivine. It demonstrates that the $Ca_{12}Al_{14}O_{33}$ still keeps its binder properties after the deposition on olivine. The catalytic activity of all sorbents/catalysts and olivine was studied in toluene steam reforming at 700 °C. The CaO/olivine and CaO–CaAl/olivine 1:2 show the best activity compared to sorbents/catalysts 1:4 and olivine. Afterwards, the best catalyst for H_2 production is CaO/olivine 1:2 however it presents the small pore volume which is related with its fast saturation and its high CO_2 selectivity, compared to CaO–$Ca_{12}Al_{14}O_{33}$/olivine 1:2. In fact, the mayenite does not improve the activity of CaO because this phase presents nor catalytic activity nor sorbent capacity. However, the mayenite phase provides the sorption properties to favors CO_2 sorption stability and is added with this purpose.

In conclusion, in order to carry out biomass gasification in a fluidized bed, CaO–CaAl/olivine 1:2 is a promising material. Firstly, thanks to the olivine the bi-functional material has a high attrition resistance. Secondly, in a fluidized bed reactor the biomass gasification process will take place in the first minutes, at which point the CaO–CaAl/olivine can reach its maximum activity, as a result of the iron oxide and sorbent phases. Thirdly, based in sorption and thermo-gravimetric analysis, the CaO–CaAl/olivine has a quite well CO_2 sorption stability, which is essential for a use in a dual circulating fluidized bed (FICFB) reactor where the carbonation–decarbonation cycles take place in the gasification and combustion zones, respectively.

References

[1] L. Di Felice, C. Courson, P.U. Foscolo, A. Kiennemann, International Journal of Hydrogen Energy 36 (2011) 5296–5310.
[2] K. Polychronopoulou, A. Bakandritsos, V. Tzitzios, J. Fierro, A. Efstathiou, Journal of Catalysis 241 (2006) 132–148.
[3] D. Świerczyński, S. Libs, C. Courson, A. Kiennemann, Applied Catalysis B: Environment 74 (2007) 211–222.
[4] H. de Lasa, E. Salaices, J. Mazumder, R. Lucky, Chemical Reviews 111 (2011) 5404–5433.
[5] A. Sarıoğlan, International Journal of Hydrogen Energy 37 (2012) 8133–8142.
[6] B. Acharya, A. Dutta, P. Basu, International Journal of Hydrogen Energy 35 (2010) 1582–1589.
[7] M. Virginie, C. Courson, D. Niznansky, N. Chaoui, A. Kiennemann, Applied Catalysis B: Environmant 101 (2010) 90–100.
[8] S. Rapagnà, M. Virginie, K. Gallucci, C. Courson, M. Di Marcello, A. Kiennemann, P.U. Foscolo, Catalysis Today 176 (2011) 163–168.
[9] M. Virginie, J. Adánez, C. Courson, L.F. de Diego, F. García-Labiano, D. Niznansky, A. Kiennemann, P. Gayan, A. Abad, Applied Catalysis B: Environment 121–122 (2012) 214–222.
[10] H. Hofbauer, R. Rauch, K. Bosch, R. Koch, C. Aichernig, Pyrolysis and Gasification of Biomass and Waste, CPL Press, Newbury Berks, U.K., 2003, pp. 527–536.
[11] Z. Abu El-Rub, E.A. Bramer, G. Brem, Industrial and Engineering Chemistry Research 43 (2004) 6911–6919.
[12] D. Świerczyński, C. Courson, A. Kiennemann, Chemical Engineering and Processing: Process Intensification 47 (2008) 508–513.
[13] J. Corella, J.M. Toledo, R. Padilla, Energy Fuels 18 (2004) 713–720.
[14] K. Matsuoka, T. Shinbori, K. Kuramoto, T. Nanba, A. Morita, H. Hatano, Y. Suzuki, Energy Fuels 20 (2006) 1315–1320.
[15] A. Reichhold, H. Hofbauer, Chemical Engineering and Processing 34 (1995) 521–527.
[16] S. Rapagnà, N. Jand, A. Kiennemann, P.U. Foscolo, Biomass and Bioenergy 19 (2000) 187–197.
[17] D. Swierczynski, C. Courson, L. Bedel, A. Kiennemann, S. Vilminot, Chemistry of Materials 18 (2006) 897–905.
[18] J.N. Kuhn, Z. Zhao, L.G. Felix, R.B. Slimane, C.W. Choi, U.S. Ozkan, Applied Catalysis B: Environment 81 (2008) 14–26.
[19] R. Rauch, C. Pfeifer, K. Bosch, H. Hofbauer, D. Świerczyński, C. Courson, A. Kiennemann, in: A.V. Bridgwater, D.G.B. Boocock (Eds.), Science in Thermal and Chemical Biomass Conversion, vol. 1, CPL Press, Newbury Berks, U.K., 2006, pp. 799–809.
[20] K. Matsuoka, T. Shimbori, K. Kuramoto, H. Hatano, Y. Suzuki, Energy Fuels 20 (2006) 2727–2731.
[21] F. Kirnbauer, V. Wilk, H. Kitzler, S. Kern, H. Hofbauer, Fuel 95 (2012) 553–562.
[22] J. Meyer, J. Mastin, T. Bjørnebøle, T. Ryberg, N. Eldrup, Energy Procedia 4 (2011) 1184–1191.
[23] C. Pfeifer, B. Puchner, H. Hofbauer, Chemical Engineering Science 64 (2009) 5073–5083.
[24] Z. Li, N. Cai, Y. Huang, H. Han, Energy Fuels 19 (2005) 1447–1452.
[25] V. Manovic, E.J. Anthony, Industrial and Engineering Chemistry Research 48 (2009) 8906–8912.
[26] Z. Li, N. Cai, Y. Huang, Industrial and Engineering Chemistry Research 45 (2006) 1911–1917.
[27] C.S. Martavaltzi, A.A. Lemonidou, Industrial and Engineering Chemistry Research 47 (2008) 9537–9543.
[28] E.Ch. Lemonidou, A.A. Vagia, Applied Catalysis A 351 (2008) 111–121.
[29] C.S. Martavaltzi, A.A. Lemonidou, Chemical Engineering Science 65 (2010) 4134–4140.
[30] C. Li, D. Hirabayashi, K. Suzuki, Fuel Processing Technology 90 (2009) 790–796.
[31] Y.R. Xie, L.H. Shen, J. Xiao, D.X. Xie, J. Zhu, Energy Fuels 23 (2009) 5199–5205.
[32] J. Delgado, M.P. Aznar, Industrial and Engineering Chemistry Research 36 (1997) 1535–1543.
[33] G. Taralas, M.G. Kontominas, Fuel 83 (2004) 1235–1245.
[34] I. Barin, Thermochemical Data of Pure Substances, VCH Verlagsgesellschaft mbh, Weinheim, Germany, 1989.
[35] C. Courson, L. Udron, D. Świerczyński, C. Petit, A. Kiennemann, Catalysis Today 76 (2002) 75–86.
[36] G.S. Grasa, J.C. Abanades, Industrial and Engineering Chemistry Research 45 (2006) 8846–8851.
[37] T.A. Milne, R.J. Evans, Biomass Gasifier Tars: Their Nature, Formation, and Conversion, National Renewable Energy Laboratory, Technical Report TP-570-25357, 1998.
[38] M.D. Brown, E.G. Baker, L.K. Mudge, Biomass 11 (1986) 255–270.
[39] J.C. Abanades, D. Alvarez, Energy Fuels 17 (2003) 308–315.
[40] H. Lu, P.G. Smirniotis, Industrial and Engineering Chemistry Research 48 (2009) 5454–5459.
[41] L. Machala, J. Tucek, R. Zboril, Chemistry of Materials 23 (2011) 3255–3272.
[42] J. Zieliński, I. Zglinicka, L. Znak, Z. Kaszkur, Applied Catalysis A 381 (2010) 191–196.

[43] H.Y. Lin, Y.W. Chen, C. Li, Thermochimica Acta 400 (2003) 61–67.
[44] W.K. Jozwiak, E. Kaczmarek, T.P. Maniecki, W. Ignaczak, W. Maniukiewicz, Applied Catalysis A 326 (2007) 17–27.
[45] K. Barcova, M. Mashlan, R. Zboril, P. Martinec, Journal of Radioanalytical and Nuclear Chemistry 255 (2003) 529–533.
[46] D. Alvarez, J.C. Abanades, Energy Fuels 90 (2005) 270–278.
[47] W. Liu, J.S. Dennis, D.S. Sultan, S.A.T. Redfern, S.A. Scott, Chemical Engineering Science 69 (2012) 644–658.
[48] N. Florin, P. Fennell, Energy Procedia 4 (2011) 830–838.
[49] C.S. Martavaltzi, A.A. Lemonidou, Microporous and Mesoporous Materials 110 (2008) 119–127.